MEASUREMENT AND ANALYSIS OF HIGH TEMPERATURE USING DISTRIBUTED FIBER OPTIC SENSOR

Yongjiao Wang[1,2], Bin Yang[2] and Lei Liang[1]

[1] National Engineering Laboratory for Fiber Optical Sensing Technology
Wuhan University of Technology, Wuhan, 430070, China

[2] School of Computer Science, University of Uuban Construction, Pingdingshan, 467036, China

EMAILS: WANGYONGJIAOAA@YEAH.NET

Abstract- In this paper the working principle and application status of distributed optical fiber temperature sensor, amplified spontaneous Raman scattering phenomenon and its time-domain characteristics are analyzed. A new measuring principle based on amplified spontaneous Raman scattering light pulse signal temperature effect is presented, and is applied to distributed optical fiber sensor systems. Noise inevitably exists in data collected by distributed optical fiber temperature sensing systems. According to the needs of high-temperature oil well testing, distributed high temperature single-mode fiber sensors and detection equipment are designed, and gives two-dimensional data of oil well temperature testing. Because of the weak Raman backwards scattered signal and serious noise disturbance, multi-resolution wavelet analysis and reconstruction method are adopted for the de-noising of testing signal.

Index terms*: Fiber optic; Sensor; Digital signal processing; Temperature control.*

I.   INTRODUCTION

The concept of distributed fiber-optic sensor system was firstly developed in 1981 by the University of Southampton [1-3]. In 1983, Hartog carried out the principle experiments of distributed fiber-optic sensor based on laser Raman Effect of liquid fiber [4-7]. The author implemented temperature testing experiment using distributed fiber optic temperature sensor, wherein an argon ion laser has been taken as light source [8-9]. In the same year, Hartog and Dakin developed distributed fiber optic temperature sensor experimental apparatus independently taking semiconductor laser as light source [10-11]. Since then, distributed fiber optic temperature sensor has been greatly developed, and a variety of sensing mechanisms have been presented [12-13, 19, 20].

The development of distributed optical fiber temperature sensor system has gone through three stages: short-range stage (2km Systems), medium-range stage (10km systems) and long-range stage (30 km Systems) [14-15, 17-18]. In some special applications, such as fire monitoring of mains power plants, explosion protection systems of coal mines and oil wells, and deformation monitoring of highways and urban rail transit systems, current long-range distributed optical fiber temperature sensor systems cannot meet the requirements of test temperature and distance; therefore, distributed optical fiber temperature measurement systems with much longer distance are urgently needed. Researches on new temperature measurement principles are to achieve this goal. Distributed optical fiber temperature sensors adopting optical fiber scattering theory can overcome the shortcomings of traditional point electronic sensors that cannot work in environments of high temperature, high pressure, corrosion, strong geomagnetic disturbances etc. It is not sensitive to electromagnetic interference and is able to withstand extreme conditions, including high temperature, high pressure and strong shock and vibration environment. Distributed optical fiber temperature sensing monitoring system exerts advantages such as wide measurement range, high spatial resolution, high accuracy and ease of automation, etc., and shows broad application prospects in wide range temperature measurements and monitoring dam seepage.

However, monitoring temperature data obtained by the distributed optical fiber temperature sensing monitoring system is inevitably adulterated with noise, thus affecting the accuracy of monitoring data. In this paper, amplified spontaneous Raman scattering phenomenon and its time-domain characteristics are analyzed according to the working principle and application

status of distributed optical fiber temperature sensors. Propose a new fiber optic temperature amplified spontaneous Raman scattering light pulse signal based on temperature effect measuring principle and apply it to distributed optical fiber sensor systems, and then discuss the experimental results and the experimental data based on the new temperature measurement principle. According to the needs of high-temperature oil well testing, distributed high temperature single-mode fiber sensors and detection equipment are designed, and gives two-dimensional data of oil well temperature testing. Because of the weak Raman backwards scattered signal and serious noise disturbance, multi-resolution wavelet analysis and reconstruction method are adopted for the denoising of testing signal. Through field testing applications, distributed optical fiber sensing technology can be used in high temperature, high pressure and strong shock and vibration environments of petrochemical, metallurgy, and electric power industry etc.

II.   THE BASIC THEORY OF WAVELET[16]

Wavelet transform [10] is to decompose a finite energy signal into a function family (wavelet basis function) resulting from the dilation and translation of a fast decay and oscillatory function (mother wavelets). A variable time-frequency window is equipped for base functions on the phase plane, in order to accommodate needs of different resolutions. In signal analysis from random noise how strong, effective extraction of information is weak, is a hot topic in current research of multi discipline. Fourier transform has been the people as the best means of signal analysis of treatment effect, but the Fourier transform is a pure frequency domain analysis method, it reflects the characteristic in the signal all the time under the whole frequency domain, and can not provide the frequency information of any local time segment, namely Fourier transform has no time-frequency localization characteristic.

2.1 The basic principle of wavelet transform

Let ψ be a finite energy function defined on $(-\infty, +\infty)$, and constitute a square integral signal space, denoted by $\psi \in L2(R)$; the resulting function family $\{\psi_{ab}\}$ can be expressed as:

$$\psi_{ab}(t) = |a|^{-0.5} \psi(\frac{t-b}{a}) \qquad -\infty < b < +\infty, a > 0 \tag{1}$$

$\psi(t)$ is called wavelet function, and $\psi_{ab}(t)$ is generated by the dilation and translation of $\psi(t)$.

a is the dilation factor, b is the translation factor. For any signal $f(i) \in L2(R)$, the continuous wavelet transform can be defined as the inner product of the signal and the wavelet basis function:

$$WT(f(t); a, b) \le f, \psi_{ab} \ge |a|^{-0.5} \int_R \psi(\frac{t-b}{a}) \, dt \quad (2)$$

Continuous wavelet transform has properties of linearity, translation invariance, retractable total variability, self-similarity and redundancy etc. In engineering, the most widely used is the dyadic wavelet transform in signal processing using wavelet transform method. Let $a = 2^1$, $b = k2^1$, then the dyadic wavelet transform of f (t) is:

$$W_f \le f(t), \psi_{j,k} \ge |2|^{-j/2} \int_R f(t)\psi(2^{-j} - k) \, dt \quad (3)$$

In the dyadic wavelet transform, scale parameters are discretized, while the translation parameters on time domain maintain continuous change.

In 1988, Mallat presented the concept of multi-resolution analysis when constructing orthogonal wavelet basis functions, with which the multi-resolution feature of wavelet have been vividly illustrated. All previous orthogonal wavelet construction methods were unified, gave out a fast orthogonal wavelet transform algorithm, namely Mallat algorithm.

Set f_k be the discrete sampling data of a signal, if $C_{o,k} = f_k$, then:

$$C_{j,k} = \sum_n C_{j-1} h_{N-2k}$$
$$D_{j,k} = \sum_n C_{j-1} g_{N-2k} \quad (4)$$
$$k = 0, 1, 2..., N-1$$

N is discrete sampling data; h and g is the filter impulse response, namely the coefficient of decomposition filter bank in each column; $C_{j,k}$ is the approximation coefficients of the signal; $D_{j,k}$ is the successive approximation of f_k in the resolution of 2^j; $D_{j,k}$ is the detail coefficient of the signal; $D_{j,k} f_k$ is the discrete detail of f_k in the resolution of 2^j. The Mallat reconstruction algorithm of the signal is:

$$C_{j-1,N} = \sum C_j h_{N-2k} + \sum D_j g_{N-2k} \quad (5)$$

h_{N-2k} and g_{N-2k} are the conjugate transposes of h_{N-2k} and g_{N-2k} respectively, and indeed the impulse response of the filter, i.e. the reconstruction filter bank coefficients.

Using Mallat algorithm, data close to the original signal can be obtained from discrete sampling signals coming through a low pass filter. Signal edge detail information is obtained after passing though a high-pass filter, so the essence of wavelet transform is a filtering operation. With the increase of the wavelet transform scale, the original signal glitches and noises can be gradually smoothed out, and the signal will overcome the noise and dominate the detail information. It is the key to extract the mutated signal characteristics to minimize the relative distortion generated by the filter.

2.2 The theory of noise reduction based on wavelet transform

It is one of the important applications of wavelet analysis to eliminate signal noise. A one-dimensional model of a signal containing noise can be expressed as:

$$s(i) = f(i) + \sigma e(i) \qquad i = 0, 1, 2, ..., n-1 \qquad (6)$$

Where, $f(i)$ is the true signal; $e(i)$ is noise; $s(i)$ is the signal containing noise. Here, a simple noise model is used to describe the process, namely let $e(i)$ be Gaussian white noise N (0,1), and the noise level be 1. In practical engineering, the effective signal manifests itself as a low-frequency signal or a stable signal, while the noise signal is manifested in high-frequency signal, so the noise cancellation process can be implemented according to the following approaches.

First, the actual signal is decomposed into wavelets. Then the high-frequency coefficient of wavelet is threshold quantization processed. Finally, according to the low-frequency coefficient of Nth layer and the quantized high-frequency coefficients of 1-Nth layers, reconstruct the signal, to eliminate the noise signal. Generally, there are 3 wavelet de-noising methods:

(1) Forced de-noising method. In this method, all the high-frequency parts of the whole structure are regarded as zero, namely, all the high-frequency parts are eliminated, and then reconstruct the signal. This method is simple to carry out, and resulted signal is relatively smooth, but it is easy to lose useful signals.

(2) Default threshold de-noising processing. In the software of Matlab, default threshold of the signal is generated using the function, and then carry out de-noising process using the wdencmp function.

(3) De-noising processing given soft or hard threshold. In the actual de-noising process, the threshold value can be obtained by empirical formula, and this threshold value is more credible than the default threshold. Details of signal decomposition and reconstruction of tree tree as shown in Figure 1.
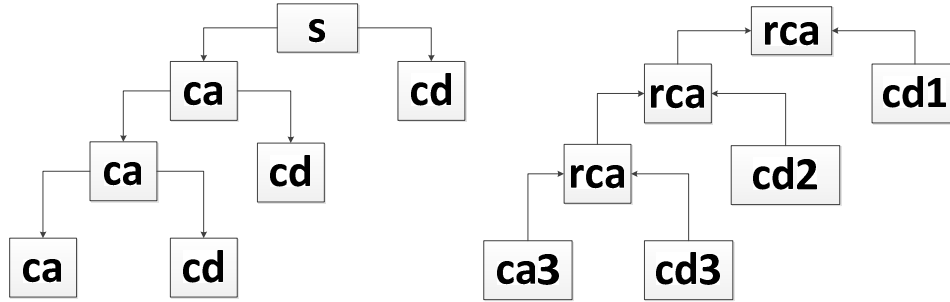

Figure 1. Wavelet decomposition tree and reconstruction tree

III. DESIGN OF TEMPERATURE CONTROL SYSTEM

3.1 Study of Brillouin scattering distributed optical fiber sensing scheme

Measurement of relationship between the Brillouin scattering frequency shift and power temperature, achieve the temperature and pressure at the same time. Theoretical and experimental studies prove that the strain temperature Brillouin frequency shift in fiber Brillouin scattering signal and power and fiber environment by linear relationship under certain conditions, it can be given by:

$$\Delta v_B = C_{vT} \cdot \Delta T + C_{v\tau} \cdot \Delta \varepsilon$$
$$\Delta P_B = C_{PT} \cdot \Delta T + C_{v\tau} \cdot \Delta \varepsilon \qquad (7)$$

Where: ΔV_B = Brillouin frequency shift; $\triangle \varepsilon$ for strain variation; $\triangle T$ for the change of temperature; C_{VT} Brillouin frequency shift temperature coefficient; $C_{v\varepsilon}$ for the Brillouin frequency shift and strain coefficient; $\triangle P_B$ for the Brillouin scattering optical power variation; C_{PT} is the temperature coefficient of Brillouin power; $C_{p\varepsilon}$ for Brillouin power strain coefficient.

The work process of the system: BOTDR laser transmitter subsystem provides the desired light and the pump pulse coherent detection of the local reference light is mainly for the whole system. Narrow linewidth laser emitted by the laser through the coupler was divided into probe

and local reference beam is the two part. The minor part into the optical frequency shifter, then as a reference signal is output to an optical mixer this topic implementation plan will take BOTDR as the basic structure, as shown in Figure 2:
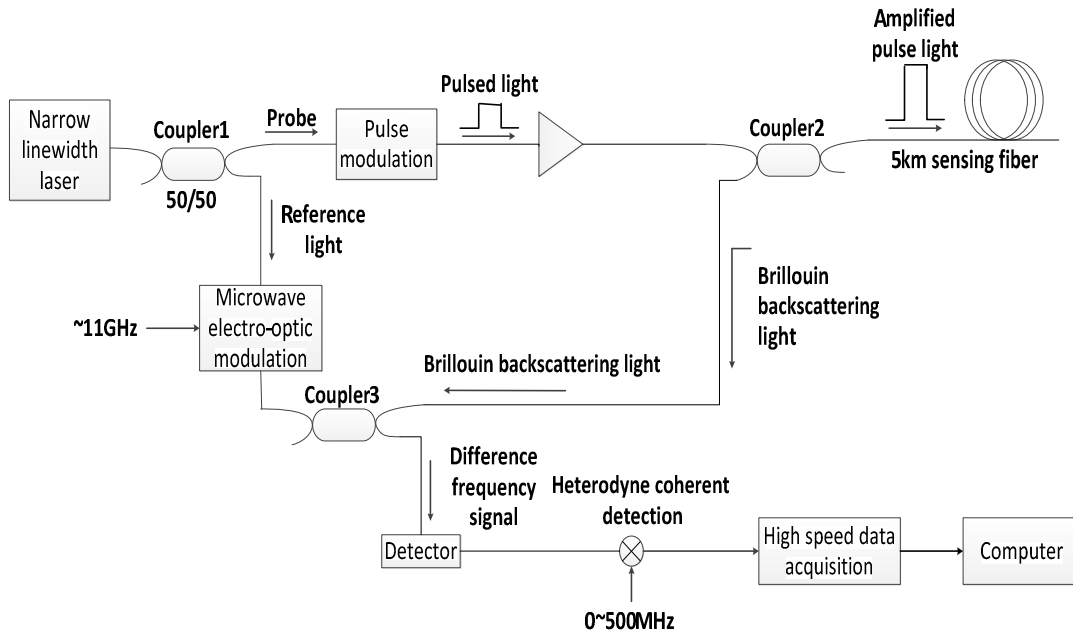

Figure 2. The basic structure of topic implementation plan

3.2 Temperature measurement principles

Distributed optical fiber temperature sensing technique is a hot research spot over the past decade. For long distance applications, most researches have focused on fiber optic temperature measurement based on light scattering mechanism. Currently, common used systems include Rayleigh scattering system based on optical fiber time domain reflection (OTDR), Raman backscatter system (ROTDR), Brillouin scattering system (BOTDR), distributed fiber sensing measurement system etc.

When laser pulse propagates in the fiber, Rayleigh scattering occurs due to the microscopic inhomogeneity of the refractive index in the fiber. In time domain, time needed for incident light returning to the incident end is t, the distance traveled by the laser pulse in the fiber is L, and $2L = V * t$, where V is the light propagation speed in the optical fiber. At t, the measured signal is the local backwards Rayleigh scattering light, the distance to the incident end is L. Using the time domain reflection technique, the loss of the optical fiber can be determined, failure point and break point can be positioned, so, it can be called fiber laser radar.

In the space domain, Rayleigh backwards scattering photon flux of the fiber is:

$$\phi_R = K_R \cdot S \cdot v_0^4 \cdot \phi_e \cdot \exp(-2\alpha_0 L) \tag{8}$$

Formula (1): Where, ϕ_e is the photon flux of the laser pulse at the incident end of the optical fiber; K_R is the coefficient related to the Rayleigh scattering cross section; v_0 is the frequency of the incident laser; S is the backwards scatter factor of the optical fiber; α_0 is the loss of the fiber at the frequency of the incident photon; L is the distance between the location and the incident end:

$$L = \frac{C \cdot t}{2n} \tag{9}$$

In frequency domain, the Raman scattered photons is divided into Stokes and anti-Stokes Raman scattering photons. The frequency of Stokes Raman scattering photon is:

$$v_s = v_0 - \triangle v \tag{10}$$

The frequency of anti-Stokes Raman scattering photon is:

$$v_\alpha = v_0 + \triangle v \tag{11}$$

Where, $\triangle v = 1.32 \times 10^{13} Hz$ is the vibration frequency of the fiber optic phonon.

Stokes Raman scattering photon flux is almost independent of temperature T:

$$\phi_s = K_s \cdot S \cdot v_s^4 \cdot \phi_e \cdot \exp[-(\alpha_0 + \alpha_s) \cdot L] \cdot R_s(T) \tag{12}$$

The anti-Stokes Raman scattering photon flux is modulated by the temperature T of the local area:

$$\phi_\alpha = K_\alpha \cdot S \cdot v_\alpha^4 \cdot \phi_e \cdot \exp[-(\alpha_0 + \alpha_\alpha) \cdot L] \cdot R_\alpha(T) \tag{13}$$

Where, K_s and K_α are factors related to Stokes and anti-Stokes Raman scattering cross sections respectively; S is the backwards scattering factor of the optical fiber; v_s and v_α are the sub-frequencies of Stokes and anti-Stokes Raman scattering photon respectively; α_0, α_s and α_α are transmission loss of incident light, Stokes Raman scattering light and anti-Stokes Raman scattering light respectively; L is the length of the fiber to be tested; $R_s(T)$ and $R_\alpha(T)$ are coefficients related to the molecular populations of fiber on low energy level and high energy level, which depends on the temperature of the fiber to be tested:

$$R_s(T) = [1 - \exp(-h\Delta v / kT)]^{-1} \tag{14}$$

$$R_\alpha(T) = [\exp(h\Delta v / kT) - 1]^{-1} \tag{15}$$

Where, h is Planck's constant; k is Boltzmann's constant.

$$\frac{\phi_\alpha}{\phi_s} = \frac{K_\alpha}{K_s} \cdot [\frac{v_\alpha}{v_s}]^4 \cdot \exp(-h\Delta v / kT) \cdot \exp[-(\alpha_\alpha - \alpha_s)L] \qquad (16)$$

Demodulate the anti-Stokes Raman scattering OTDR curve with Stokes Raman scattering OTDR curve, according to formula (16), the temperature T of a point on the fiber at a distance L from the incident end can be obtained.

Here, we propose a new fiber optic temperature amplified spontaneous Raman scattering light pulse signal based on temperature effect measuring principle and apply it to distributed optical fiber sensor systems.

3.3 Software and hardware design and debugging of control system

Following the interrupt subroutine module design ideas: first, to determine whether the timer 1 interrupt, if it is interrupted, the other cause is returned; if the timer interrupt is generated by 1, 2ms first started counting; to Article 20ms, A/D began sampling; and then transferred to PI closed loop control subroutine calculate output pulse time, also is the solid state relay turn-on time.

After the completion of the hardware and the software program is compiled, you can connect to the DSP simulator for hardware debugging. Its main purpose is to synthesize each part of the design function, the realization of system control. This system mainly includes the main program, A/D conversion subroutine, interrupt service program, general I/O port and the PI closed loop control algorithm program. Timer 1 interrupt subroutine flow chart was shown in Figure 3. After the completion of the hardware and the software program is compiled, you can connect to the DSP simulator for hardware debugging. Its main purpose is to synthesize each part of the design function, the realization of system control.
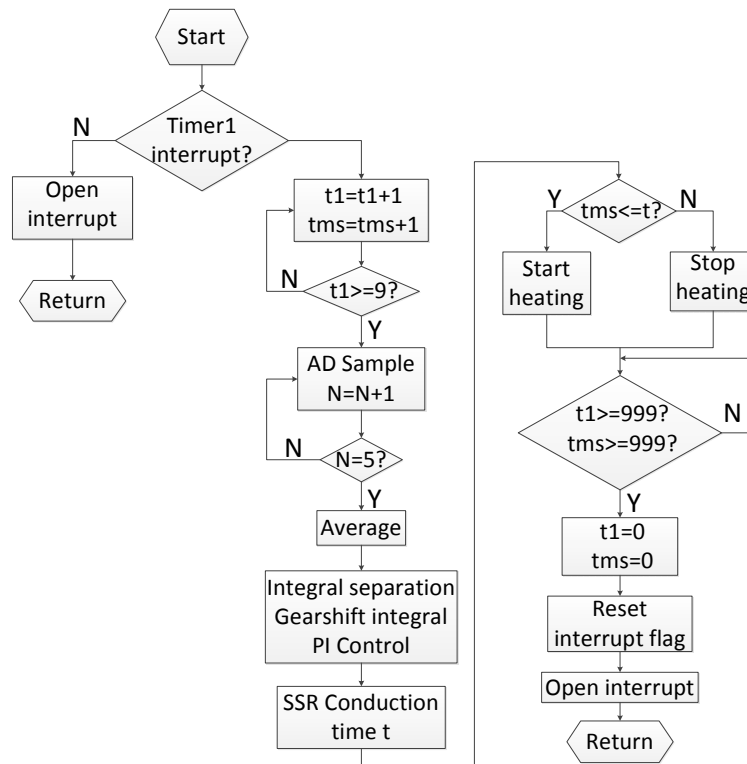
Figure 3. Timer 1 interrupt subroutine flow chart

IV. RESULT AND ANALYSIS

In most cases, ordinary optical fibers with epoxy or plastic outer layers are not applicable in high-temperature environments. The trigger laser work, every time after the trigger, by the pulse laser light emitted into the sensing fiber, optical fiber Brillouin scattering signal at each point on the generated, propagating along the fiber is returned to the injection end, through a directional coupler output at the output is detected by a series of scattering wave show wide, repeated cycles of the waveform and the trigger pulse is the same.

4.1 The validation of the model

In order to make the fiber can be widely used in the fields of oil, gas, coal and other exploration and production works with high temperature environments; it must be coated with proper refractory metals, such as chrome, aluminum, copper, etc. Optical fibers used in this article have been coated with chrome according to special process. Then the fiber is protected by stainless steel capillary armor (outer sleeve diameter is 26 mm), which is filled with lubricating oil, able to withstand high temperature and high pressure of steam injection wells. Meanwhile,

during the testing process of steam injection wells, lubricators are installed. According to the tensile strength and the outer diameter of the fiber, heavier rods and connectors have been manufactured and connected to the lower end of the capillary, so that the fiber can reach the predetermined depth in the heavy oil wells.
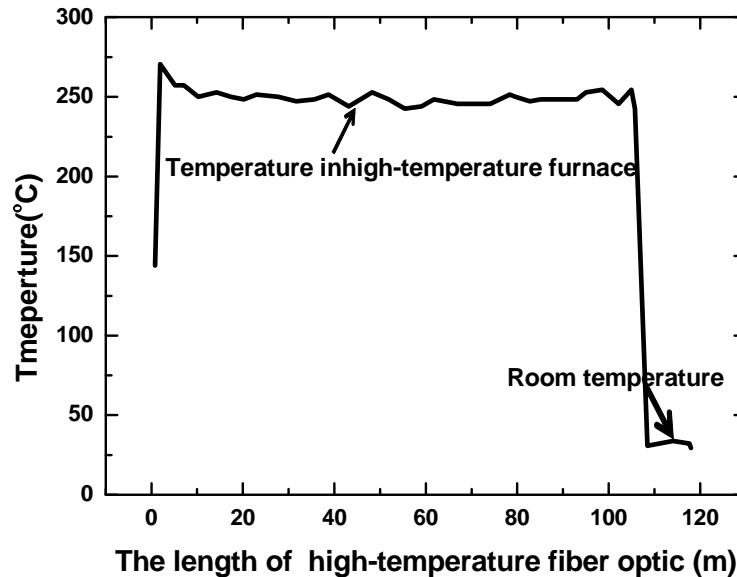

Figure 4. High-temperature fiber optic sensing system in high-temperature furnace

Figure 4 shows the long-term test results of high-temperature fiber optic sensing system in high-temperature furnace. The distributed optic fiber temperature sensing system developed in this paper is applied for single-mode fibers with long measuring distance, large measuring range. The technical parameters are listed: temperature measuring depth: 0~8km; Temperature range: -15~350℃; Temperature Range resolution: 15 m; Measurement Accuracy: ±2℃; Test time: ≤60 s; work pressure: ≤35MPa.

After denoising, get the intensity of optical signals on the frequency of the corresponding per meter, is the number of discrete points, must get the Brillouin spectrum based on these points, to find the maximum intensity of Brillouin frequency shift corresponding to the frequency spectrum curve, then according to the corresponding relationship between the frequency shift and temperature, can calculate the corresponding temperature. Three spline curve fitting, is an ordered series of discrete points, an interpolation method with a smooth curve in order to connect. Three order spline interpolation function has many good properties: such as smoothness, maintaining a continuous two order derivatives, which have very high application value in engineering and mathematics application.

4.2 The experiment of high temperature

After being calibrated using high-temperature furnace, the distributed optical fiber temperature measurement system has been tested in oilfield wells. The end of the fiber is descended into 1050m insider the well, and the total length of the fiber is 2 000 m. After long-term on-line measurement, the original Stokes Raman signal, the anti-Stokes Raman scattered signal, and the demodulated temperature signal are obtained, as shown in Figure 5 and Figure 6.
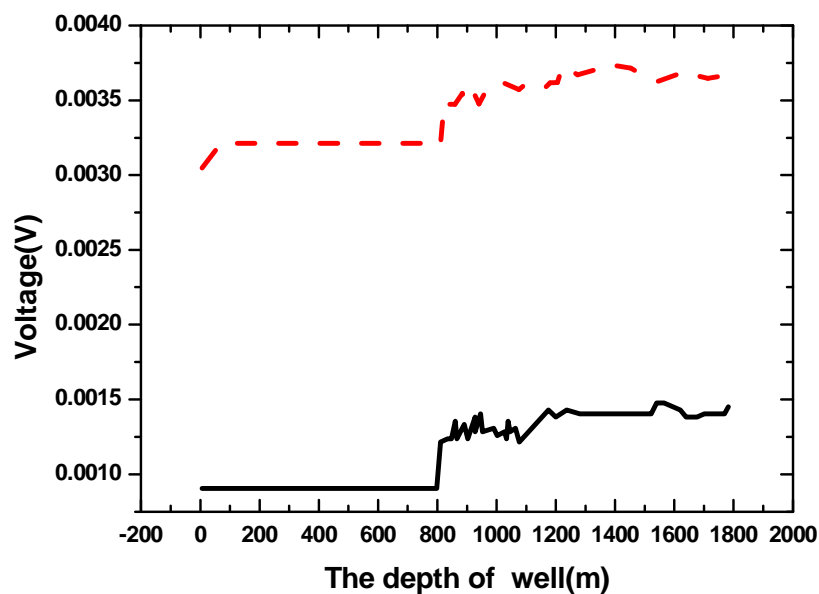

Figure 5. Stokes Raman and anti-Stokes Roman scattered signal

As shown in Figure 6, with the increase of depth, the temperature is ascended. At depth100m and 500m insider the well, the temperature is suddenly increased. The reason is that there are four inclined wells near the test site, and interaction between formation temperatures is generated because of changes in the structure after the injection of steam.
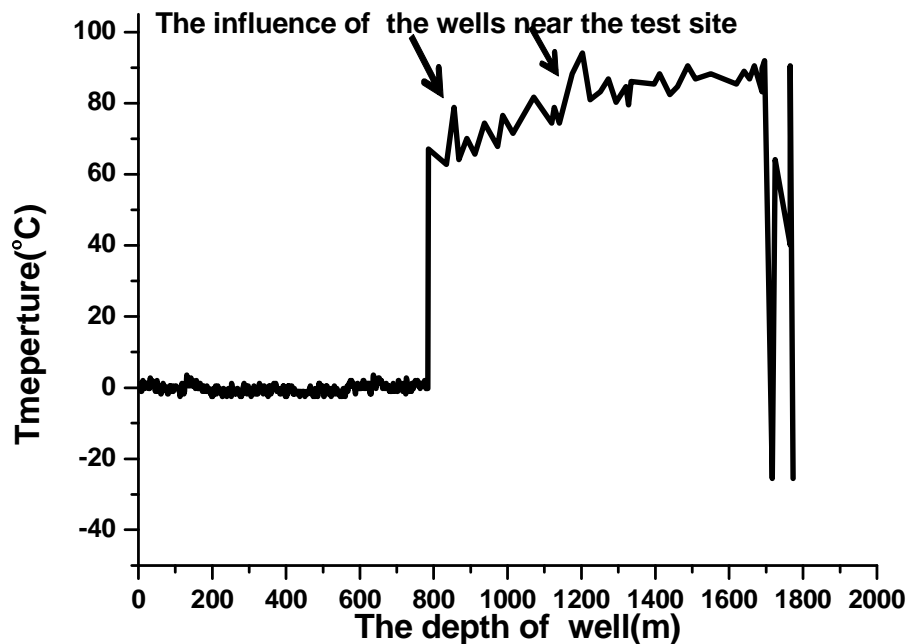
Figure 6. The original signal of well temperature test

Furthermore, even after the digital cumulative averaging processing, the noise in the original signal of well temperature test is still relatively large due to external interference. Therefore, in order to improve the measurement accuracy, the signal should be further processed to improve the signal-to-noise ratio.

4.3 Case of high temperature wells test signal analysis

Raman backwards scattering signal in distributed temperature measurement system is weak and contains a number of random noises (mostly having white noise characteristics) that are far greater than the magnitude of the Raman scattering signal. The signal-to-noise ratio of the signal after photoelectric conversion is so low that almost all useful temperature information is buried in noises. Besides, there are various inevitable energy loss in the return process of the scattering light, resulting in the fact that the intensity of the Raman scattering light at the proximal end is stronger than that of the distal end, while the intensity of noises remain unchanged. Useful temperature signal is relatively stable and is mainly concentrated in the section of low frequency, while noises are distributed over the entire frequency range. Therefore, it plays a key role to improve the signal-to-noise ratio for the measurement of temperature.

In terms of de-noising methods, there are median filtering, low-pass filtering, Fourier transform, etc., but useful part of the signal will be filtered by these methods. As a multi-

resolution analysis method, wavelet transform has an adaptive window, and has good resolution for both of time and frequency. Practical applications have proved that it is helpful for the improvement of measurement accuracy and signal-to-noise ratio to de-noise temperature measurement signals with this approach.

Specific process using wavelet analysis method for signal filtering and de-noising is listed: (1) Select wavelet form. Here wavelet is selected, it is an orthogonal wavelet function with compact support with good regularity, and is able to separate high-frequency part of the signal to low-frequency part. (2) Select wavelet decomposition level, and calculate the wavelet decomposition of signal S to the Nth layer (value of N should make the number of maxima of signal modulus dominate the total number). In this paper, take N = 4 and 6 for comparative analysis. (3) Quantify the threshold of wavelet high-frequency coefficients. Here the de-noising threshold is selected using the Mini/maxi Principle. (4) Reconstruct according to the changed wavelet coefficients, and finally get a de-noised signal.
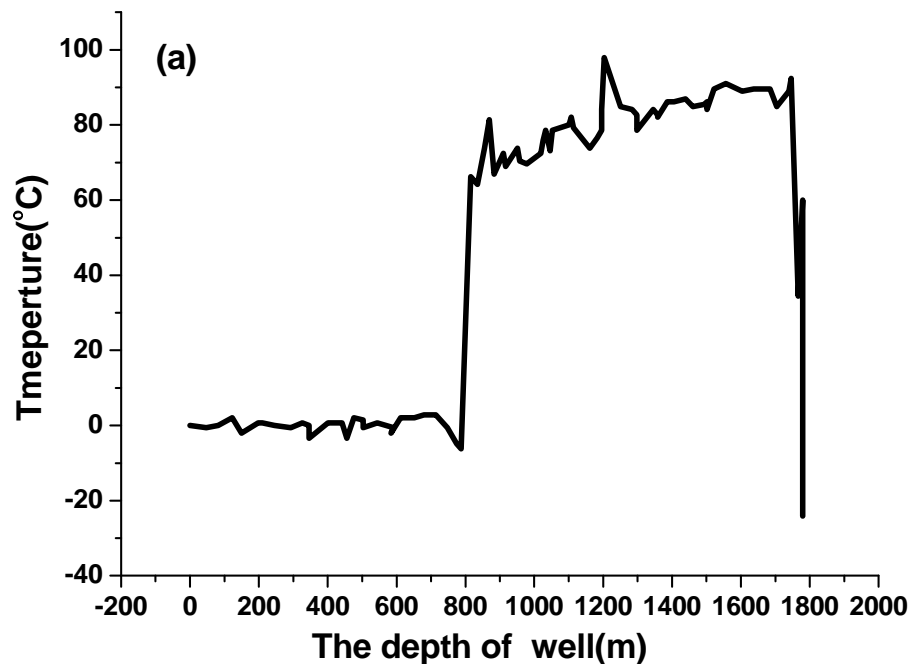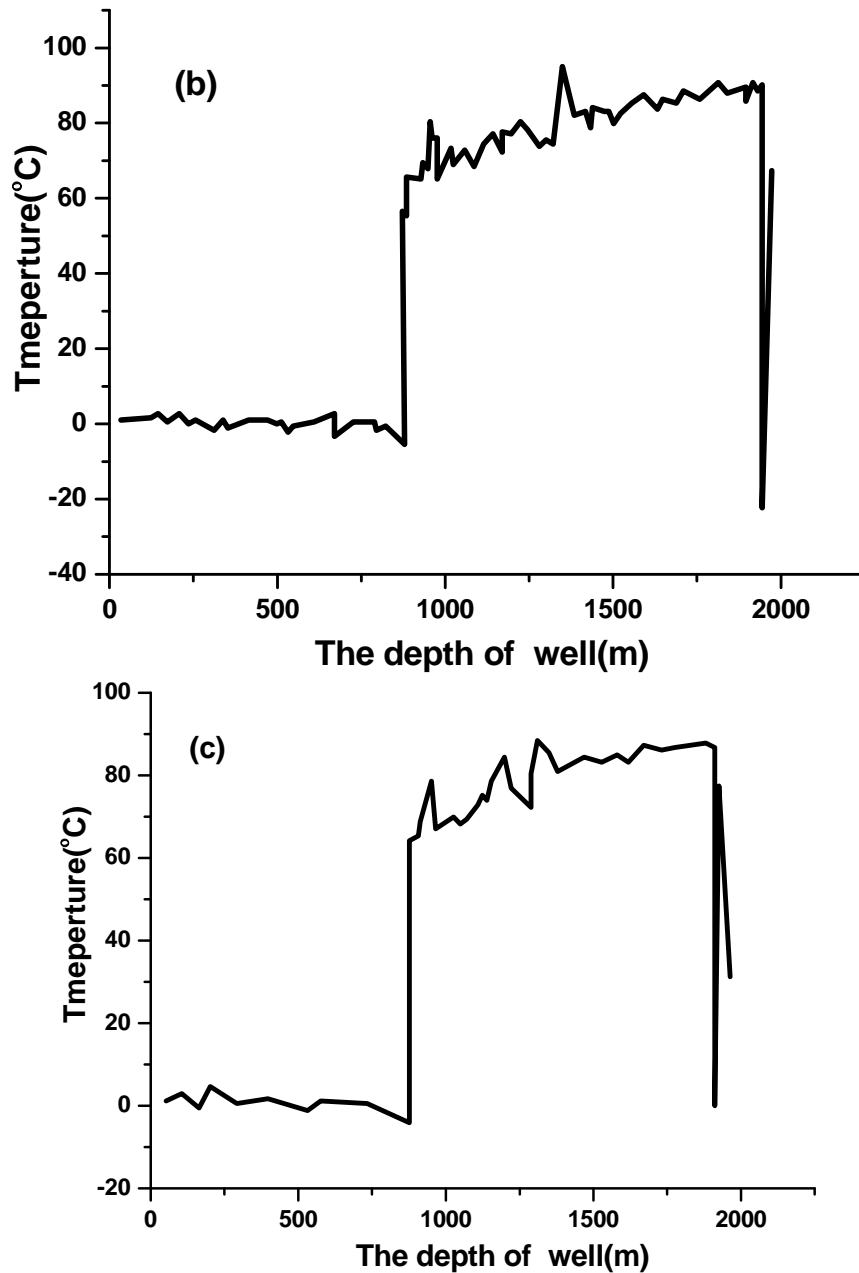
Figure 7. The reconstructed temperature signals

The reconstructed temperature signals with 6-layer wavelet decomposition and 4-layer wavelet decomposition are shown in Figure 7 (a) and 7 (b). Figure 7 (c) shows the reconstructed temperature signal with 6-layer wavelet decomposition with larger threshold. As can be seen by comparison, the wavelet de-noising method can significantly improve the signal-to-noise ratio and improve the accuracy of the temperature signal.

V.   CONCLUSIONS

Using the distributed optical fiber temperature sensing system presented in this paper, full-field long-distance temperature measurement has been realized in high-temperature and high-pressure environments. A wavelet multi-scale resolution theory is proposed to de-noise the measured temperature signal and to improve the signal-to-noise ratio, the effect of which is obvious. In this paper, according to the working principle and application status of distributed optical fiber temperature sensor, amplified spontaneous Raman scattering phenomenon and its time-domain characteristics are analyzed. A new measuring principle based on amplified spontaneous Raman scattering light pulse signal temperature effect is presented, and is applied to distributed optical fiber sensor systems. According to the needs of high-temperature oil well testing, distributed high temperature single-mode fiber sensors and detection equipment are designed, and gives two-dimensional data of oil well temperature testing. Because of the weak Raman backwards scattered signal and serious noise disturbance, multi-resolution wavelet analysis and reconstruction method are adopted for the de-noising of testing signal, which has significant economic and social benefits.

VI. REFERENCES

[1] Nath, D.K., Sugianto, R., Finley, D., Fiber-optic distributed-temperature-sensing technology, 2006 SPE/IADC INDIAN Drilling Technology Conference and Exhibition, pp.9-18, 2006.

[2] J.P.Dakin, Distributed fiber-optic sensor system, Optoelectronics Research Centre, pp. 377-385.

[3] Juarez, J.C et al., Distributed fiber-optic intrusion sensor system, Journal of Lightwave Technology, vol.23, no.6, pp.2081 - 2087, 2005.

[4] Ma X, Chang J, Wang L, et al. Using Multiple Reference Points in Raman Based Distributed Temperature Sensor for Eliminating DC Interference, Sensors Journal, vol.14, no.1, pp. 295 - 301, 2014.

[5] Yonghao Xu, Xianfeng Chen,and Yu Zhu, High Sensitive Temperature Sensor Using a Liquid-core Optical Fiber with Small Refractive Index Difference Between Core and Cladding Materials, Sensors , vol.8, no.3, pp.1872–1878, 2008.

[6] Minakuchi, S.; Takeda, N.; Takeda, S.-I.; Nagao, Y.; Franceschetti, A.; Liu, X. Life cycle monitoring of large-scale CFRP VARTM structure by fiber-optic-based distributed sensing. Compos. Part A 2011, 42, 669–676.

[7] López-López M, García-Ruiz C. Infrared and Raman spectroscopy techniques applied to identification of explosives. TrAC Trends in Analytical Chemistry, 2014, 54: 36-44.

[8] Xu, M.G.; Archambault, J.-L.; Reekie, L.; Dakin J.P. Discrimination between strain and temperature effects using dual-wavelength fibre grating sensors. Electron. Lett. 1994, 30, 1085–1087.

[9] Damien Kinet et al., Fiber Bragg Grating Sensors toward Structural Health Monitoring in Composite Materials: Challenges and Solutions, Sensors, vol.14, pp.7394-7419, 2014.

[10] Kodriano Y, Schmidgall E R, Benny Y, et al. Optical control of single excitons in semiconductor quantum dots. Semiconductor Science and Technology, 2014, 29(5): 053001.

[11] Vo T D, He J, Magi E, et al. Chalcogenide fiber-based distributed temperature sensor with sub-centimeter spatial resolution and enhanced accuracy. Optics Express, 2014, 22(2): 1560-1568.

[12] Saxena M K, Raju S, Arya R, et al. Optical fiber distributed temperature sensor using short term Fourier transform based simplified signal processing of Raman signals. Measurement, 2014, 47: 345-355.

[13] Challener W A. Multiparameter fiber optic sensing system for monitoring enhanced geothermal systems. General Electric Global Research, 2014.

[14] Kersey A D. A review of recent developments in fiber optic sensor technology. Optical fiber technology, 1996, 2(3): 291-317.

[15] He J, Zhou Z, Ou J. Simultaneous measurement of strain and temperature using a hybrid local and distributed optical fiber sensing system. Measurement, 47: 698-706, 2014.

[16] Podrouzek J, Bucher C, Deodatis G. Identification of critical samples of stochastic processes towards feasible structural reliability applications. Structural Safety, 2014, 47: 39-47.

[17] S.C.Mukhopadhyay and S.K.Pal, "Temperature Analysis of Induction Motors Using a Hybrid Thermal Model with Distributed Heat Sources", Journal of Applied Physics, June 1998, Vol 83, No. 1, pp 6368-6370.

[18] A. Mason, S. Wylie et al.., flexible e-textile sensors for real-time health monitoring at microwave frequencies, International Journal on Smart Sensing and Intelligent Systems, vol. 7, no. 1, pp. 31 – 47, 2014.

[19] Jianping He, Zhi Zhou, Jinping Ou, Simultaneous measurement of strain and temperature using a hybrid local and distributed optical fiber sensing system, Measurement, vol.47, pp.698–706,2014.

[20] Gabriele Bologninia, Arthur Hartogb, Raman-based fibre sensors: Trends and applications, Optical Fiber Technology, vol.19, no.6, pp.678–688, 2013.